International Journal of Mechanical, Industrial and Aerospace Sciences
ISSN: 2517-9950
Vol:5, No:2, 2011

Comparison of Detached Eddy Simulations with Turbulence Modeling

Muhammad Amjad Sohail, Prof. Yan Chao, Mukkarum Husain

***Abstract*—**Flow field around hypersonic vehicles is very complex and difficult to simulate. The boundary layers are squeezed between shock layer and body surface. Resolution of boundary layer, shock wave and turbulent regions where the flow field has high values is difficult of capture. Detached eddy simulation (DES) is a modification of a RANS model in which the model switches to a subgrid scale formulation in regions fine enough for LES calculations. Regions near solid body boundaries and where the turbulent length scale is less than the maximum grid dimension are assigned the RANS mode of solution. As the turbulent length scale exceeds the grid dimension, the regions are solved using the LES mode. Therefore the grid resolution is not as demanding as pure LES, thereby considerably cutting down the cost of the computation. In this research study hypersonic flow is simulated at Mach 8 and different angle of attacks to resolve the proper boundary layers and discontinuities. The flow is also simulated in the long wake regions. Mesh is little different than RANS simulations and it is made dense near the boundary layers and in the wake regions to resolve it properly. Hypersonic blunt cone cylinder body with frustrum at angle 5^o and 10^o are simulated and there aerodynamics study is performed to calculate aerodynamics characteristics of different geometries. The results and then compared with experimental as well as with some turbulence model (SA Model). The results achieved with DES simulation have very good resolution as well as have excellent agreement with experimental and available data. Unsteady simulations are performed for DES calculations by using duel time stepping method or implicit time stepping. The simulations are performed at Mach number 8 and angle of attack from 0^o to 10^o for all these cases. The results and resolutions for DES model found much better than SA turbulence model.

***Keywords*—**Detached eddy simulation, dual time stepping, hypersonic flow, turbulence modeling

I. Introduction

THE DES treatment of turbulence is aimed at the prediction of separated flows, thin and dense shock and boundary layers at unlimited Reynolds numbers and at a manageable cost. The claim is that it soundly combines fine-tuned Reynolds-Averaged Navier– Stokes (RANS) technology in the boundary layers, and the simple power of Large-Eddy Simulation (LES) in the separated regions [1]. In the RANS regions, the turbulence model has full control over the solution, but it is used within a plausible envelope. In the LES region, little control is left to the model, the larger eddies are resolved, and grid refinement directly expands the range of scales in the solution, and therefore the accuracy of the nonlinear interactions available to the largest eddies [2]. The computing-cost outcome is favorable enough that a challenging Separated flow, namely an airfoil at high angles of attack and fairly high Reynolds numbers, was treated quite successfully on personal computers [3]. The present author simulated a lot of varieties of supersonic and hypersonic laminar and turbulent flows by using laminar Navier stokes and RANS approaches [4-6]. The current author implemented the above mentioned approaches on laminar hypersonic flows and turbulent supersonic and hypersonic flows and got the desired results. For hypersonic aircraft reentry vehicles mostly the flow is turbulent and the body is moving at high angles of attack [7, 8] so flow separation and thin and dense boundary layer is obvious. The boundary layers are also squeezed between shock waves and body surfaces. So it is essential ingredients to properly capture the shock wave and resolution of boundary layers. Flow is also rapidly separating in such types of flows. There is need to properly resolve the all these phenomenon. DES is a three-dimensional, time-dependent approach which properly resolves the above mentioned phenomena by using hybrid philosophy of RANS and LES approaches on the expense of little increase in cost. The present study deals with the detail implementation of time dependent DES approach and RANS approaches. First the RANS approach using Sparllart Almaras turbulent model is used and the aerodynamics characteristics are calculated for cone-cylinder and frustrum configurations. Then time dependent DES approached is used by using implicit solver and implicit time stepping (dual time steeping formulation) is used to simulate the hypersonic flow at Mach number 8. The second order Euler backward time stepping is used for the same. The finite volume and multiblock implicit solver is used for these calculations. Finally the simulated results are compared with the available experimental as well as theoretical

II. Geometrical Models

In the present investigation, Three different models have been used, namely (a) blunt cone with after body (b) blunt cone with after body and 5^o frustum and (c) blunt cone with after body with 10^o frustum, as shown in Fig.1 The first test model (blunt cone with after body) has been chosen for its simple design and represents AGARD configuration, HB-1

Muhammad Amjad Sohail is PhD student from Beijing University of Aeronautics and Astronautics Beijing China (phone: 0086-13120491221; e-mail: masohailamer@ yahoo.com).

Prof. Yan Chao is professor from Beijing University of Aeronautics and Astronautics Beijing China (phone: 0086-13501200881; e-mail: chyan@vip.sina.com@ yahoo.com).

Mukkarum Husain is PhD student from Beijing University of Aeronautics and Astronautics Beijing China (phone: 0086-13120491221; e-mail: mrmukkarum@yahoo.com).

(Hypervelocity Ballistic model). The first part of the model is a blunt cone which has an apex angle of 41◦ and length of 40.6mm. The second part of the model is the cylinder of 51mm outer diameter and a length of 186mm. The model has a spherical nose radius of 15mm. The second and third test model (Blunt cone with after body and frustum) represents a simple AGARD configuration, HB-2. The geometry of the blunt cone remains the same and the length of the cylinder is reduced to 111mm with the outer diameter of 51mm. The frustum has an axial length of 75mm with a semi-vertex angle of 5◦ and 10°. For these three configurations, the total length of the model has been kept the same in order to maintain the exact L/D (i.e., length to diameter) ratio of the model. The details and test conditions are mentioned in reference [9]

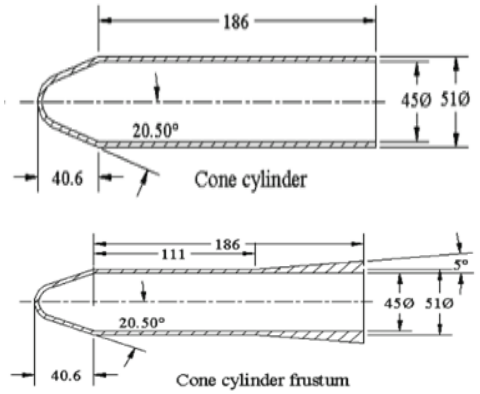

Fig: 1 Geometrical Model

III. Mesh Generation

The algebraic method is used to generate three-dimensional boundary-fitted grids for blunt cone configurations. The height of the first grid next to the body is controlled, and the grids near to the body are normalized to achieve y+ less than 1. The H-H and C-type boundary- fitted grids are generated at first in order to simulate the aerodynamic forces accurately. The mesh for Detached Eddy simulation is created very carefully. In shock wave region and corner expansion and compression regions and wake regions is meshed with very high accuracy so that the expansion ratio should be remained below 1.2. detailed study of Mesh generations for detached eddy simulations is given in reference [10]

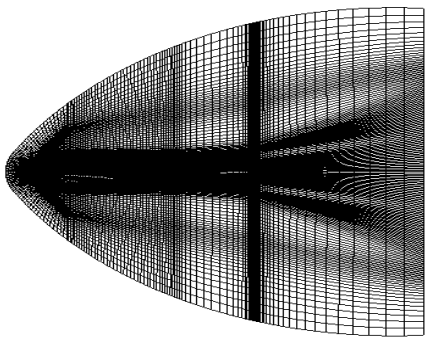

Fig: 2 Generation of mesh

IV. Governing Equations and Turbulence Models

A. Governing Equations

The system of governing equations for a single-component fluid, written to describe the mean flow properties, is cast in integral Cartesian form for an arbitrary control volume V with differential surface area dA as follows:

$$\frac{\partial}{\partial t}\int_V W dV + \iint [F - G].dA = \int_V H dV \qquad (1)$$

Where the vectors W, F and G are defined as:

$$W = \begin{bmatrix} \rho \\ \rho u \\ \rho v \\ \rho w \\ \rho E \end{bmatrix}, F = \begin{bmatrix} \rho u \\ \rho vu + P\hat{i} \\ \rho vv + P\hat{j} \\ \rho vw + P\hat{k} \\ \rho vE + Pv \end{bmatrix}, G = \begin{Bmatrix} 0 \\ \tau_{xi} \\ \tau_{yi} \\ \tau_{Zi} \\ \tau_{ij} v_j + q \end{Bmatrix}$$

Vector H contains source terms such as body forces and energy sources.

Here ρ, v, E, and p are the density, velocity, total energy per unit mass, and pressure of the fluid, respectively. T is the viscous stress tensor, and q is the heat flux.

Total energy E is related to the total enthalpy H by

$$E = H - p/\rho \qquad (2)$$

Where $H = h + \frac{|v|^2}{2}$

B. Turbulence Model

To calculate the turbulent flows the SA turbulent model is used here. The transported variable in the Spalart-Allmaras model, $\tilde{\nu}$, is identical to the turbulent kinematic viscosity except in the near-wall (viscous-affected) region. The transport equation for $\tilde{\nu}$ is

$$\frac{\partial}{\partial t}(\rho\tilde{\nu}) + \frac{\partial}{\partial x_i}(\rho\tilde{\nu}u_i) = G_\nu + \frac{1}{\sigma_{\tilde{\nu}}}\left[\frac{\partial}{\partial x_i}\left\{(\mu + \rho\tilde{\nu})\frac{\partial\tilde{\nu}}{\partial x_j}\right\} + C_{b2\rho}\left(\frac{\partial\tilde{\nu}}{\partial x_j}\right)^2\right] - Y_\nu + S_{\tilde{\nu}} \qquad (3)$$

Where G_ν is the production of turbulent viscosity and Y_ν is the destruction of turbulent viscosity that occurs in the near-wall region due to wall blocking and viscous damping. $\sigma_{\tilde{\nu}}$ and C_{b2} are constants and ν is the molecular kinematic viscosity $S_{\tilde{\nu}}$ is a user-defined source term

C. DES Model

In the DES approach [11-14], the unsteady RANS models are employed in the near-wall regions, while the filtered versions of the same models are used in the regions away from the near-wall. The LES region is normally associated with the core turbulent region where large turbulence scales play a dominant role. In this region, the DES models recover the respective subgrid models. In the near-wall region, the respective RANS models are recovered so we can say DES is the hybrid model of LES and RANS. The standard Spalart-Allmaras model uses the distance to the closest wall as the definition for the length scale d, which plays a major role in determining the level of production and destruction of turbulent viscosity as given respectively.

$$\tilde{S} = S + \frac{\tilde{\nu}}{k^2 d^2} f_{v2} \qquad (4)$$

$$Y_\nu = C_w \rho f_w \left(\frac{\tilde{\nu}}{d}\right)^2 \qquad (5)$$

$$r = \frac{\tilde{\nu}}{\tilde{S} k^2 d^2} \qquad (6)$$

The DES model, as proposed by Shur et al. [9] replaces d everywhere with a new length scale $\tilde{d}$, defined as

$$\tilde{d} = \min\left(d, C_{des}, \Delta\right) \qquad (7)$$

Where the grid spacing, Δ , is based on the largest grid space in the x, y, or z directions forming the computational cell. The empirical constant C_{des} has a value of 0.65.

D. DES Model

The implicit-time stepping method (also known as dual-time formulation) is used here for the calculation of detached eddy simulation in the implicit formulation. Density based implicit solver is used for both RANS and LES simulations with SA and K-ω SST turbulence modeling. Preconditioned pseudo-time-derivative term is used here

$$\frac{\partial}{\partial t}\int_V W dV + \Gamma \frac{\partial}{\partial \tau}\int_V Q dV + \iint [F - G].dA = \int_V H dV \qquad (8)$$

Where t denotes physical-time and τ is a pseudo-time used in the time-marching procedure. If as $\tau \to \infty$, the second term on the left side of Equation (4) vanishes. The time-dependent term in Equation (4) is discretized in an implicit fashion by means of either a first- or second-order accurate, backward difference in time. The dual-time formulation is written in semi-discrete form as follows which is second order accurate for these simulations:

$$\left[\frac{\Gamma}{\Delta\tau} + \frac{\varepsilon_0 \partial W}{\Delta t \partial Q}\right]\Delta Q^{K+1} + \frac{1}{V}\iint [F - G].dA = H - \frac{1}{\Delta t}\left(\varepsilon_0 W^k - \varepsilon_1 W^n + \varepsilon_2 W^{n-1}\right) \qquad (9)$$

Physical time step Δt is limited only by the level of desired temporal accuracy. The pseudo-time-step $\Delta\tau$ is determined by the CFL condition of the time-marching scheme. Normally physical time step is taken as 0.00001 to 0.001s and 500 time steps are taken for these computations. The convective fluxes are calculated by using AUSM+ and all other equations like turbulence etc are taken as second order accurate.

V. Results and Discussion

A. Test case 1

The test conditions for these simulations are M_∞ is taken as 8 P_∞ 212 pa and T_∞ is 149 and the convergence criteria for these simulations is taken as for continuity and energy equations is 10^{-4} and for x,y,z velocities and others quantities 10^{-5} to 10^{-6}. For turbulent model the steady state simulations are performed but for DES computations unsteady time dependent dual time stepping implicit solver is used. First model cone-cylinder is simulated at Mach number 8 with sparllart almaras turbulent model and DES with SA model and angle of attack 0^o to 10^o. The simulated results for angle of attack 8^o are shown in figure (3). Contours of Mach number, density total pressure and temperature are shown for DES computations.

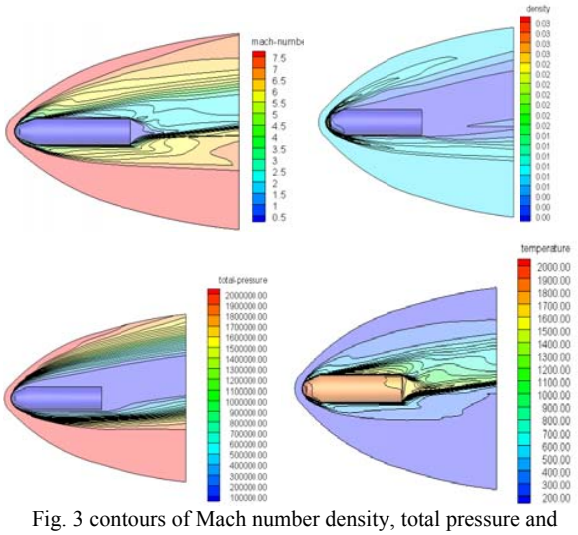

Fig. 3 contours of Mach number density, total pressure and temperature for cone-cylinder at angle of attack 8^o and Mach number for DES computations

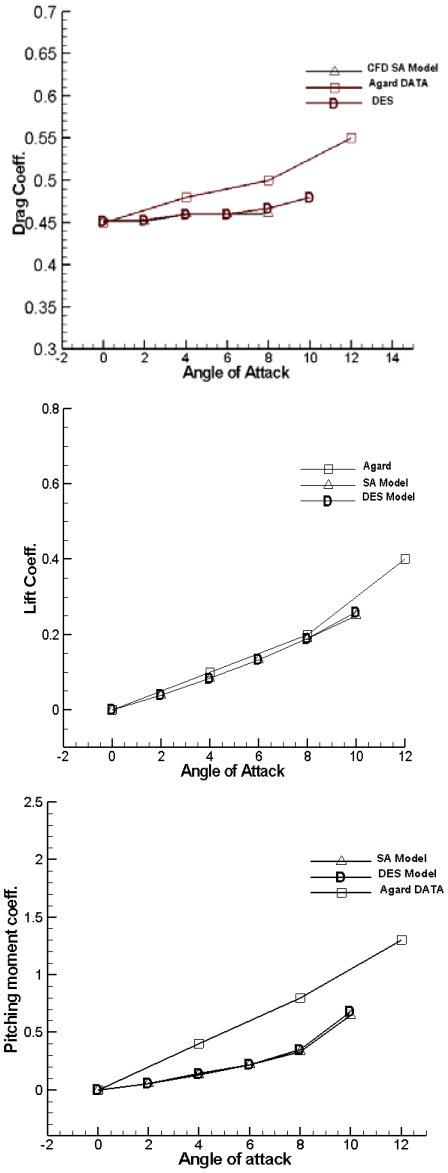

Fig. 4 Drag, lift and pitching moment coefficients v angle of attack for cone-cylinder configuration

In the above figure (4) aerodynamics characteristics are compared for DES, SA and AGARD data. The results are found in good agreement

B. Test case 2

The second configuration which is simulated is cone-cylinder frustrum with 5° angle of flare or frustrum. The same configuration is simulated at 0 to 10° angle of attack. In figure (5) contours of Mach number, density, temperature and pressure at angle of attack 10° are shown. Both for SA model and DES model shock waves are properly captured and the reverse flow and flow separation is properly resolved. In figure (6) vorticity magnitude contour are shown for DES model. Vortices and vortex shedding phenomenon is shown clearly.

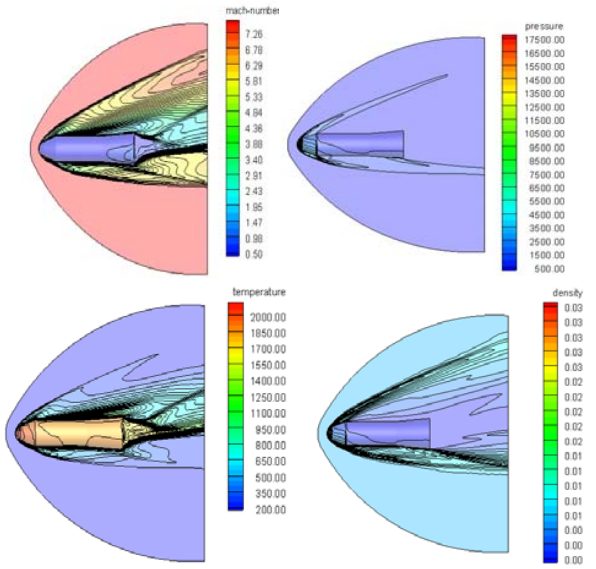

Fig: 5 cone-cylinder frustrum 5 deg DES contours of mach, pressure, temperature and density at mach 8 angle of attack 10°

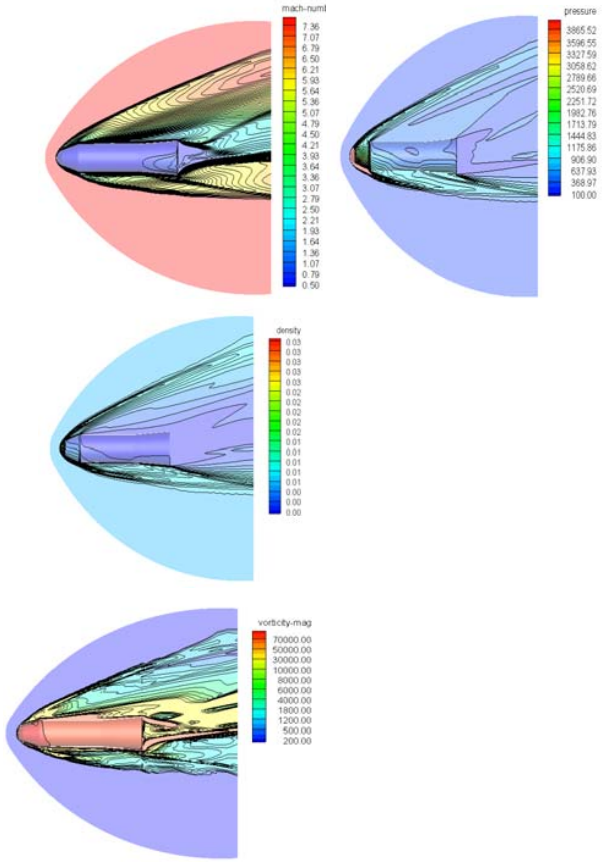

Fig. 6 cone-cylinder frustrum 5 deg SA Model contours of mach, pressure, density and density at mach 8 angle of attack 10°

In figure (7) the comparison of contours for both SA model and DES model are show. From the contours it is clearly

shown that how the Mach number and viscosity contours resolutions are varies between two models SA and DES. DES resolutions are much better than SA model. In figure (8) resolution and shock capturing with mesh refinement is shown for DES model.

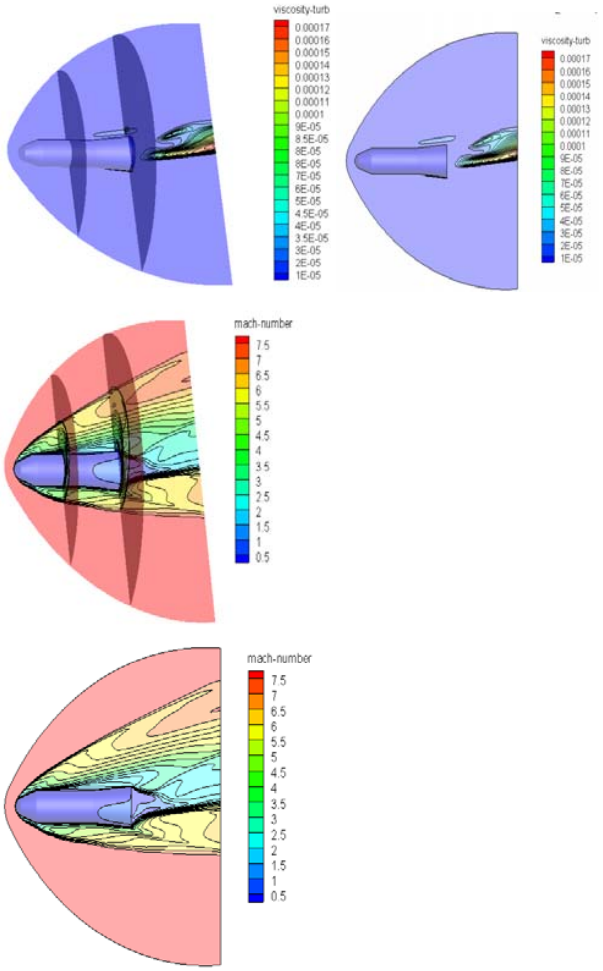

Fig: 7 cone-cylinder frustrum 5 deg DES and SA Model contours of turbulent viscosity Mach (at mach 8 angle of attack 10^o

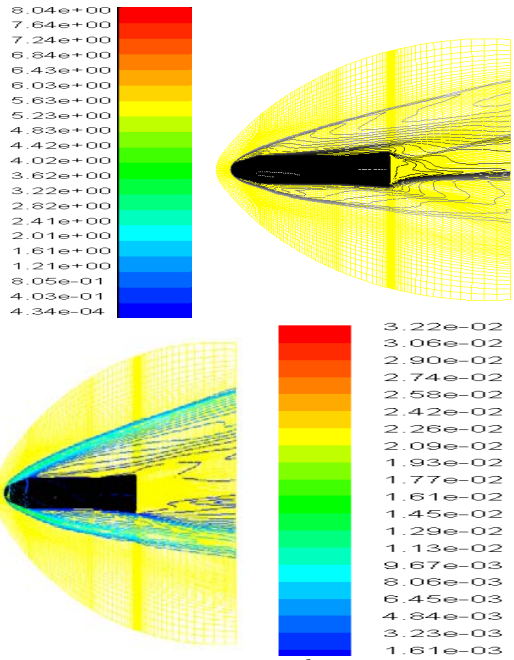

Fig. 8 cone-cylinder frustrum5^o contours of Mach number, density, at mach 8 and angle of attack 6^o for DES

In figure (9) computed results for drag. Lift and pitching moment coefficients are shown for cone-cylinder frustrum 5^o configuration. As the angle of attack increased then the same are also increased as shown in graph. The results are compared with the results of agard data.

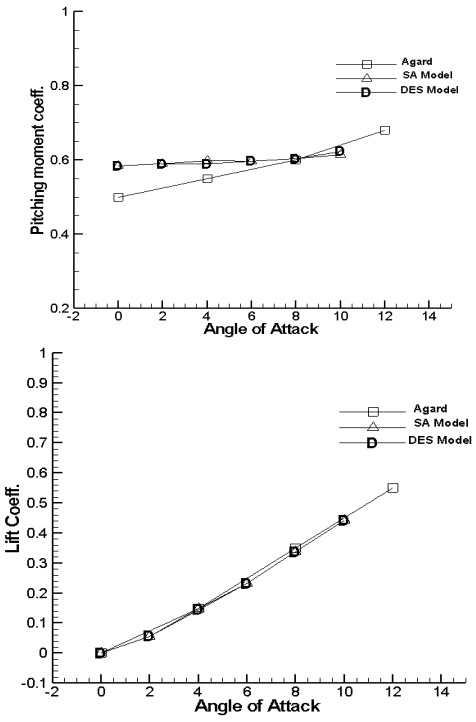

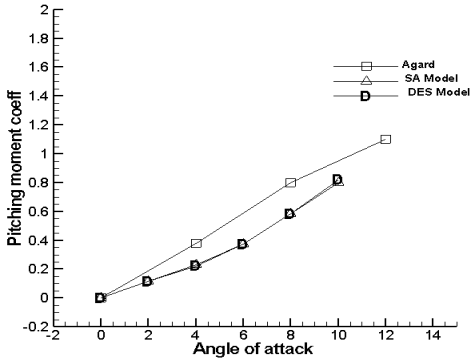

Fig: 9 Drag, lift and pitching moment coefficients v angle of attack for cone-cylinder frustrum 5^o configuration

C. Test case 3

The last configuration is cone-cylinder frustrum 10^o flare angle. The results are obtained at Mach number 8 and the contours of Mach number, density, temperature and total pressure are shown in the figure (10). The figure (11) shows that when the frustrum angle is increased then the lift and pitching moment coefficients are increased the results for both configurations 5^o and 10^o frustrum are compared.

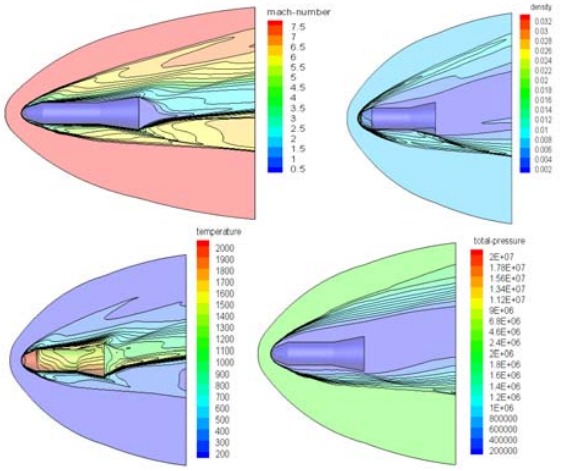

Fig: 10 frustrum 10^o contours of Mach number density temperature and total pressure at mach 8 angle of attack 8^o

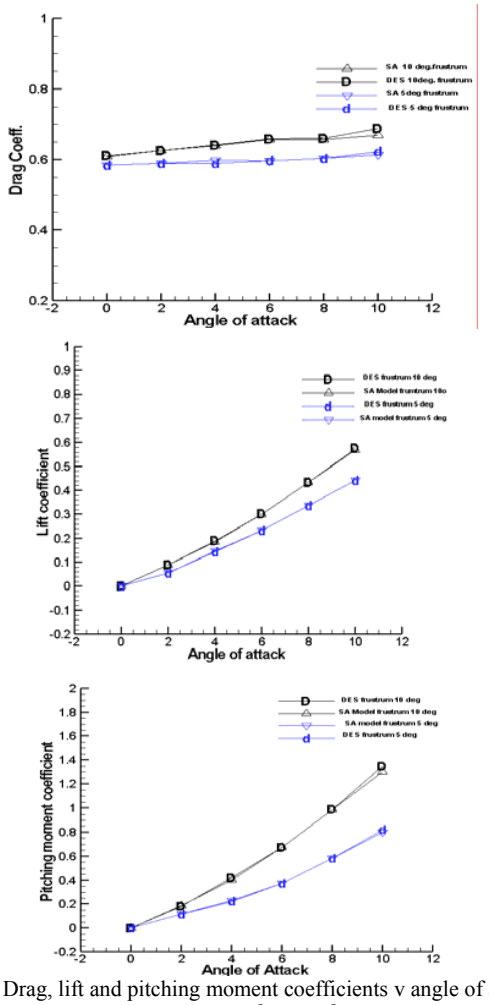

Fig: 11 Drag, lift and pitching moment coefficients v angle of attack for cone-cylinder frustum 5^o and 10^o configuration

VI. Conclusion

DES simulations are performed at Mach number 8 by using SA model and dual time stepping implicit formulations. The results are compared with standard SA turbulent model and Agard data. The Turbulent model SA resolved the boundary layers and high pressure gradient flows and shows acceptable results in boundary layers and wake expansion compression and separated region with y+ value less than 1. But when the same configurations are simulated with DES model then the wall regions and wake regions are properly resolved the turbulent viscosity is properly resolved by DES model by using the RANS and LES version of the same. The mesh is little modified for the LES part of the DES model to properly resolve the turbulent viscosity where the turbulent length scales is increased. So from these computations we have concluded that with the little expense of cost the DES models gives the better results for highly turbulent flows by using the RANS and LES nature of the model.

. .

ACKNOWLEDGMENT

The first author is very thankful to the Pakistan higher Education commission (HEC) for the funding of his PhD and other support to accomplish the project. He is also very thankful to Professor Yan Chao for his kind guidelines for the same.

REFERENCES

[1] Spalart, P.R., Jou, W.-H., Strelets, M. and Allmaras, S.R., Comments on the feasibility of LES for wings, and on a hybrid RANS/LES approach. In: Liu, C. and Liu, Z. (eds), Advances in DNS/LES, Proceedings of 1st AFOSR International Conference on DNS/LES, Ruston, LA,August 4–8. Greyden Press, Columbus, OH (1997) pp. 137–147.

[2] Spalart, P.R., Strategies for turbulence modelling and simulations. Internat. J. Heat Fluid Flow,to appear.

[3] Shur, M., Spalart, P.R., Strelets, M. and Travin, A., Detached-eddy simulation of an airfoil at high angle of attack. In: Rodi, W. and Laurence, D. (eds), 4th International Symposium on Engineering TurbulenceModelling and Measurements, Corsica, May 24–26. Elsevier, Amsterdam (1999) pp. 669–678.

[4] Muhammad Amjad Sohail , Muhammad yamin Younis "applications of High order low dessipitive shcme on hypersonic flow field by using min mode limiter"CFP1070K-PRT, ISBN=11-4244-8101-9 Singapore 2010.

[5] Muhammad Amjad Sohail et al" Effect of Turbulence Modeling on Aerodynamics characteristics of a conventional tailed finned missile configurations" CFP1070K-PRT, ISBN=11-4244-8101-9 Singapore 2010.

[6] Muhammad Yamin Younis., Muhammad Amjad Sohail, Tawfiqur Rahman, Zaka Muhammad, Saifur Rahman Bakaul" Applications of AUSM+ Scheme on Subsonic, Supersonic and Hypersonic Flows Fields" World Academy Of Science, Engineering and Technology Issue 73 January 2011

[7] J PRoos, F.W. and Kegelman, J.T., "Aerodynamic Characteristics of Three Generic Forebodies at High Angles of Attack," AIAA Paper 91-0275, January, 1991.).

[8] Jason M. Merret* and Michael B. Bragg" X-38 AERODYNAMICS DURING RAPID PITCH UP" University of Illinois at Urbana-Champaign Urbana, IL 61801AIAA 2003-3526.

[9] S. Saravanan • G. Jagadeesh • K. P. J. Reddy" Aerodynamic force measurement using 3-componentaccelerometer force balance system in a hypersonic shock tunnel" Shock Waves (2009) 18:425–435 DOI 10.1007/s00193-008-0172-8.

[10] Philipe R. Spalart "Young's persons guide for detached eddy simulations Grid generations" NASA/CR-2001-211032

[11] M. Shur, P. R. Spalart, M. Strelets, and A. Travin. Detached-Eddy Simulation of an Airfoil at High Angle of Attack. In 4th Int. Symposium on Eng. Turb. Modeling and Experiments, Corsica, France, May 1999.

[12] Scott A. Morton" High Reynolds Number Detached-Eddy Simulations of Vortex Breakdown Over A 70 Degree Delta Wing"

[13] B. CARUELLEa, and F. DUCROSb" Detached-Eddy Simulations of Attached and Detached Boundary Layers" International Journal of Computational Fluid Dynamics, December 2003 Vol. 17 (6), pp. 433–451

[14] ANDREI TRAVIN, MICHAEL SHUR, MICHAEL STRELETS and PHILIPPE SPALART" Detached-Eddy Simulations Past a Circular Cylinder" Flow, Turbulence and Combustion 63: 293–313, 1999